Neuromagnetic Decoding of Simultaneous Bilateral Hand Movements for Multidimensional Brain–Machine Interfaces

Abdelkader Nasreddine Belkacem, Shuichi Nishio, Takafumi Suzuki, Hiroshi Ishiguro, and Masayuki Hirata

***Abstract*— To provide multidimensional control, we describe the first reported decoding of bilateral hand movements by using single-trial magnetoencephalography signals as a new approach to enhance a user's ability to interact with a complex environment through a multidimensional brain–machine interface. Ten healthy participants performed or imagined four types of bilateral hand movements during neuromagnetic measurements. By applying a support vector machine (SVM) method to classify the four movements regarding the sensor data obtained from the sensorimotor area, we found the mean accuracy of a two-class classification using the amplitudes of neuromagnetic fields to be particularly suitable for real-time applications, with accuracies comparable to those obtained in previous studies involving unilateral movement. The sensor data from over the sensorimotor cortex showed discriminative time-series waveforms and time-frequency maps in the bilateral hemispheres according to the four tasks. Furthermore, we used four-class classification algorithms based on the SVM method to decode all types of bilateral movements. Our results provided further proof that the slow components of neuromagnetic fields carry sufficient neural information to classify even bilateral hand movements and demonstrated the potential utility of decoding bilateral movements for engineering purposes such as multidimensional motor control.**

***Index Terms*— Android, bilateral movements, brain-machine interface, magnetoencephalography, motor imagery, SVM classification, voluntary motor control.**

Manuscript received August 28, 2017; revised February 13, 2018 and April 24, 2018; accepted May 8, 2018. Date of publication May 15, 2018; date of current version June 6, 2018. This work was supported in part by the ImPACT Program of the Council for Science, Technology and Innovation (Cabinet Office, Government of Japan), in part by the "Development of BMI Technologies for Clinical Application" through the Strategic Research Program for Brain Sciences by AMED, in part by the "Research and Development of Technologies for High Speed Wireless Communication From Inside to Outside of the Body and Large Scale Data Analyses of Brain Information and Their Application for BMI" from NICT, and in part by KAKENHI funded by the Japan Society for the Promotion of Science under Grant 26282165. *(Corresponding author: Masayuki Hirata.)*

A. N. Belkacem is with the Global Center for Medical Engineering and Informatics, Endowed Research Department of Clinical Neuroengineering, Osaka University, Osaka 565-0871, Japan (e-mail: belkacem011@hotmail.com).

S. Nishio is with Hiroshi Ishiguro Laboratories, Advanced Telecommunications Research Institute International, Kyoto 619-0288, Japan.

T. Suzuki is with the Center for Information and Neural Networks, National Institute of Information and Communications Technology, Osaka 565-0871, Japan.

H. Ishiguro is with the Department of System Innovation, Graduate School of Engineering Science, Osaka University, Osaka 560-8531, Japan.

M. Hirata is with the Global Center for Medical Engineering and Informatics, Endowed Research Department of Clinical Neuroengineering, Osaka University, Osaka 565-0871, Japan, and also with the Department of Neurosurgery, Graduate School of Medicine, Osaka University, Osaka 565-0871, Japan (e-mail: mhirata@nsurg.med.osaka-u.ac.jp).

This paper has supplementary downloadable material available at http://ieeexplore.ieee.org, provided by the author.

Digital Object Identifier 10.1109/TNSRE.2018.2837003

I. Introduction

A BRAIN-MACHINE interface (BMI) for motor control is a system based on decoding brain activity data from the motor cortex in the human forebrain to offer an alternative to physiological motor pathways. Such a system is able to send commands from the brain to a machine by using motor signals generated via voluntary motor control or motor imagery tasks in subjects performing certain body movements or imagining these movements without using the brain's normal output pathways of peripheral nerves and muscles, respectively. The brain signals for BMIs are measured with either invasive or noninvasive techniques.

For decades, most studies have focused on discriminating unilateral actual/imagined movements such as right or left hand/finger/toe grasping and tongue movement [1]–[3]. This decoding of unilateral movements has been well studied and used in controlling machines (computers and cursors [4]–[7], robots and prostheses [8]–[10], etc.) to achieve a high reliability in noninvasive BMIs on the basis of electroencephalography (EEG) and magnetoencephalography (MEG) signals. Regarding the cortical activation of unilateral movements, previous studies have shown that in both brain hemispheres there are typical movement-related cortical potentials or fields as well as certain oscillatory changes in the frequency bands, such as the alpha (8-13 Hz), beta (13-30 Hz) and gamma (>30 Hz) bands. Generally, a diffuse power decrease in the alpha and beta bands has been observed in the sensorimotor area, whereas a more focal power increase in the gamma band has been observed in the motor area. Furthermore, previous noninvasive EEG or MEG studies have demonstrated that the decoding accuracy of a 2-class classification for two types of voluntary or imaginary body movements is significantly higher than that expected by chance. The accuracy has been found to vary from 60% to 80% using a sensor or source decoding level [4]–[19]. In contrast, the mean multi-class classification accuracy of movement decoding that has been achieved from the same part of the body has been less than or approximately equal to 60% in most BMI studies [20]–[23].

A dimension of control or degree of freedom is a critical issue for achieving a high performance in motor BMIs in a complex real-time interaction in a more realistic environment. In this case, decoding bilateral hand movements or hand gestures may be an initial step toward increasing dimensionality and achieving a continuous and multidimensional control of multiple devices (e.g., wheelchair and robotic arm). This type of multidimensional BMI system would require higher dimensional control and naturalistic BMI tasks. In addition, unilateral and bilateral movements activate different parts of the brain [24]–[28]. When patients perform or imagine bilateral movements during rehabilitation exercise sessions, patients activate more areas of the brain and therefore maximize the neuroplastic benefits [29]. Furthermore, simultaneous bilateral movements (e.g., contralateral and ipsilateral hand movements) require a greater overall activation of muscle contraction and therefore probably require the firing of a greater number of cortical cells [24], [25]. Because the topography of brain activity is well known regarding unilateral movements [30], [31], it is of interest to clarify the spatiotemporal frequency distribution of neural activity during simultaneous bilateral hand movements. In addition, people simultaneously use their hands bilaterally for doing different tasks in daily life. However, to date, analyzing human brain activity during simultaneous bilateral hand movements has not been reported in detail. This type of analysis may offer a better understanding of the neural correlates of bilateral hand movements, which remain unclear. Only a few studies based on functional magnetic resonance imaging (fMRI) measurements have offered a better understanding of the neural correlates of uni- and bi-manual finger presses [32] and bimanual anti-phase and in-phase movements [33]. Furthermore, decoding bilateral movements would also provide multidimensional control in multifunctional augmentative and alternative communication systems. Regarding unilateral movements, previous BMI studies based on sensorimotor amplitudes and rhythms have used electroencephalograms (EEGs), magnetoencephalograms (MEGs), or electrocoticograms (ECoGs) to distinguish between the actual/imagined movement and the rest state (e.g., right hand grasping vs. relaxing position of the left hand (no motion), and left hand grasping vs. relaxing position of the right hand). Only a few studies have added a case of bilateral movements, such as closing (grasping) bilateral hands or simultaneously moving bilateral fingers [21], [23]–[26]. None of these studies have attempted to decode four types of simultaneous bilateral hand movements (e.g., R-Close vs. L-Open: closing a right hand vs. opening a left hand, R-Open vs. L-Close: opening a right hand vs. closing a left hand, R/L-Close: closing both hands, and R/L-Open: opening both hands). In addition, the bilateral hand movement is one of the simplest paradigms to achieve using a multidimensional BMI system. In this study, to investigate the feasibility of extending the dimensionality of BMI commands, we utilized neuromagnetic oscillatory modulation to analyze and decode the brain activity associated with four types of real and imagined bilateral hand movements.

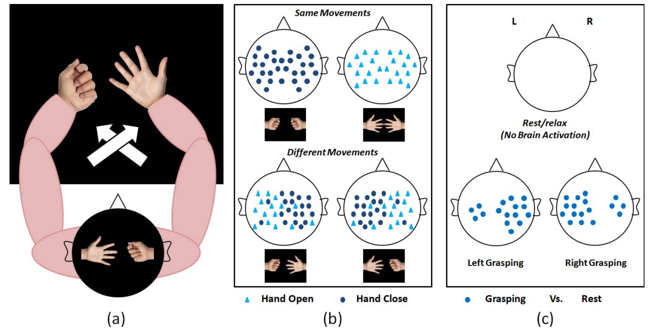

Fig. 1. The characteristic R2 distribution of a subject's uni- and bi-lateral hand movements, on the basis of a time series and event-related desynchronization around the sensorimotor cortex. (a) Experimental paradigm of performing and imagining uni- and bi-lateral hand movements. (b) Brain activation associated with bilateral movements, according to our hypothesis. (c) Brain activation associated with unilateral movements, according to previous studies showing strong contralateral activation and minimal ipsilateral activation.

In this paper, we describe a novel multidimensional MEG-based BMI approach, focusing on decoding and exploring the similarities and differences in sensorimotor activity during motor execution and motor imagery of bilateral hand movements by using a noninvasive measurement. We chose to decode both real and imagined movements in this BMI study because the brain activity involved in imagined movements (i.e., motor imagery-related activity) observed in healthy people is quite different from the brain activity observed in paralyzed people. In particular, patients who have undergone a hand amputation (i.e., phantom movement-related activity) demonstrate brain activity during imagined movements that is similar to that during real movements [34]. In addition, we used MEG in the present study because this technique has several advantages in analyzing neurophysiological signals, compared with EEG and fMRI. MEG is the noninvasive measurement of the magnetic fields outside the head, which provides direct information about the activity of the cortical neurons; MEG has a higher spatial resolution than EEG and has a broader spatial coverage than an ECoG. MEG can directly record neural activity with a higher temporal resolution than fMRI. Several previous MEG studies have demonstrated that magnetic fields preceding movement frequently show bilateral patterns of activation even for unilateral movements [35]–[38]. In addition, brain areas with similar activity patterns, such as time series, are likely to communicate and sharing information, especially if the time series of the two brain areas are highly correlated. Therefore, we hypothesized that the brain activation could be clarified on the basis of a time series analysis and certain time-frequency analyses by using MEG measurements while the subjects' perform tasks or

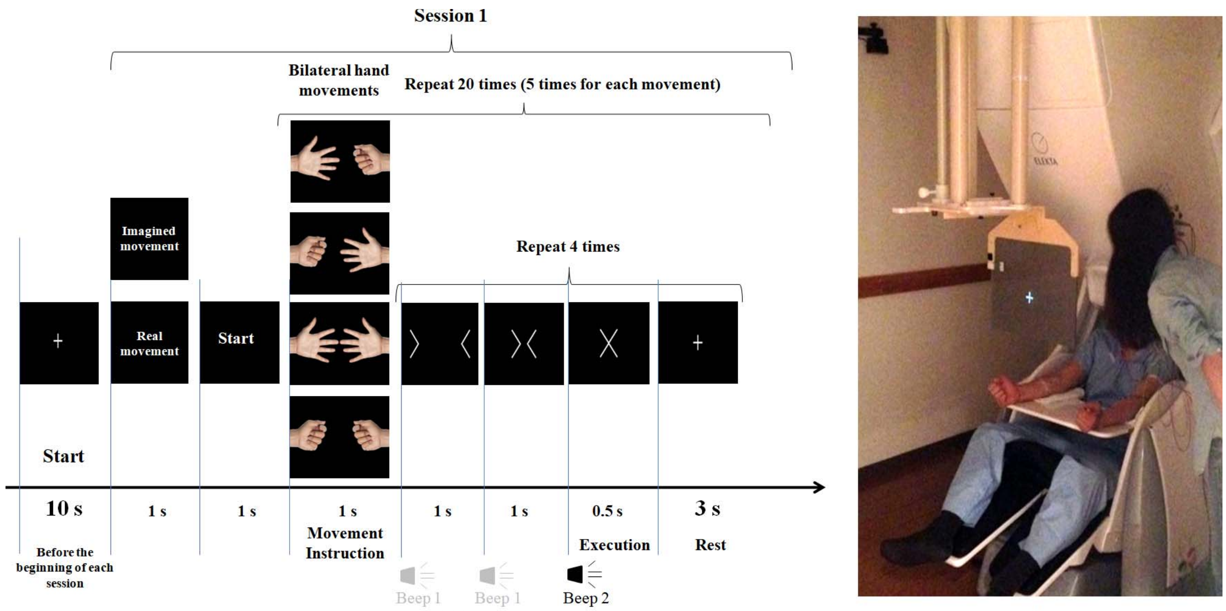

(a) (b)

Fig. 2. Experimental bilateral hand movement paradigm. (a) Subjects performed real and imagined bilateral hand movements in the same sequence. First, one of the movement types, i.e., grasping or opening, was presented on the screen in front of the subject. Then, the subject moved the right hand as instructed upon the presentation of the execution cue. Each movement type was repeated four times. Each trial consisted of the following four phases; the rest phase, instruction phase, preparation phase, and execution phase. During the rest phase, a white fixation cross "+" was presented for 3 s. During the instruction phase, an image of a bilateral hand movement was presented for 1 s. Then, during the preparation phase, two timing cues ("$>$ $<$" and "$><$") were presented one at a time, each for 1 s, to aid the subjects in preparing for the execution of the real or imagined movements. During the execution phase, the subjects performed the real or imagined movement as requested during the instruction phase after the appearance of the execution cue "$\times$." (b) MEG setup used during the real and imagined bilateral movements.

imagine bilateral movements (see Fig. 1). In this study, when subjects performed or imagined bilateral movements, the magnitude of neuromagnetic fields and the frequency power of sensorimotor activities were either increased or decreased in both brain hemispheres; these phenomena are termed event-related magnetic field (ERF) for the magnetic fields, event-related power increase (i.e., event-related synchronization, ERS) and event-related power decrease (i.e., event-related desynchronization, ERD) for the frequency power. Using these event-related activity characteristics, support vector machine (SVM) decoders were able to distinguish among the four bilateral movements.

II. Materials and Methods

A. Participants

Ten healthy volunteers (3 males and 7 females, 22-45 years of age) participated in the present study. Clear written informed consent was obtained from all the participants, who were informed in detail about the purpose and possible consequences of the experiment. The present study was approved by the Ethics Committee at Osaka University Hospital (No. 15123), and the experimental protocol was carried out in accordance with the latest version of the Declaration of Helsinki.

B. Experimental Paradigm and Protocol

MEG recording and MRI were performed at the Center for Information and Neural Networks (CiNet, Osaka, Japan). Neuromagnetic brain activity was measured with an augmented 360 high-density MEG scanner with 360 SQUID detectors surrounding the head housed in a magnetically shielded room (Elekta Neuromag TRIUX system; Elekta Oy, Helsinki, Finland). This 360-channel MEG system was composed of 306 planar sensors (204 gradiometers and 102 magnetometers) and 54 additional vertical sensors. The planar gradiometers provided sensitivity to sources close to the sensor array, whereas the magnetometers provided sensitivity to distant sources, including sources originating from a small head.

The participant was in a sitting position (see Fig. 2(b)), and a projection screen was fixed in front of the eyes. Visual stimuli were shown on the screen with a visual stimulus presentation system (Presentation, Neurobehavioral Systems, Albany, CA, USA) and a projector ($12.5 \times 16 \times 20''$) outside the shielded room. The participants were instructed to grasp or open both the right and left hands once according to the execution cues given visually and aurally. Regarding the experimental paradigm, four classes of bilateral movements (both grasping, both opening, right grasping/left opening, right opening/left grasping) were presented on the screen, and 10 MEG recording sessions were conducted. Each session included 20 movements for each class. Based on [11] and [12], the same class of movement was repeated 4 times during both the real and imagined sessions to allow the participants to easily perform the imagined movements (i.e., while performing the tasks, the participants were asked to quickly move both hands once-only at the same time, after the execution cue). The presentation order of the movement types was randomized. The participants were instructed to perform the imagined or actual movements without moving any other body parts, to avoid both muscle and head motion artifacts. In addition, the experimental paradigm and protocol were designed to enable the participants to kinesthetically perform the indicated motor imagery task rather than relying on visual imagery, while avoiding any motion during the imagery task. To reduce fatigue, we asked participants to take 10-min to 20-min breaks between the first five random sessions and the rest sessions. The schematic of the overall experimental paradigm is shown in Fig. 2(a).

Furthermore, a 3 T structural MRI scan was performed to more clearly obtain detailed images of the head and brain structures in slices for each subject. During the MEG recording and MRI scanning, we measured certain reference points. These reference points were used to co-register the MEG sensor positions to voxel coordinates of the anatomical data. An iterative closest points (ICP) algorithm was used to refine this sensor/anatomy registration. The recorded MRI data were converted using FreeSurfer software (Martinos Center software, http://surfer.nmr.mgh.harvard.edu/) into a format suitable for uploading on the Brainstorm software (http://neuroimage.usc.edu/brainstorm), and we then aligned the MEG data with the individual anatomical data. The acquisition of individual anatomical MRIs of participants in this study is desirable because the source localization is part of the planned analysis.

C. Data Acquisition and Preprocessing

Neuromagnetic activity was sampled at 1000 Hz, after which the temporal extension of the signal space separation method (tSSS) was used to suppress noise and artifacts generated by the sensors and sources of interference located very close to the MEG sensors. Because the spatial filtering used in this study was based directly on Maxwell's equations, the operation can be called Maxwell filtering; hence, we used MaxFilter 2.2 software to calculate the tSSS. A bandpass filter from 0.5 to 100 Hz and a 60-Hz notch filter were applied using Brainstorm software [39] to reduce some DC and high frequency noises and eliminate AC line noise. In addition, muscular activities were recorded using 8 electromyogram (EMG) electrodes positioned on the flexor and extensor pollicis longus to measure hand flexion and extension during the performance of bilateral movements. Thus, to obtain the exact onset of the execution of real movement, we used EMG signals as a trigger instead of using the onset time, on the basis of the execution of the visual stimulus "×". After the presentation of the execution cue, robust EMG amplitudes were observed during the real movement but not during the imagined movement (see Supplementary Fig. 2). For voluntary movements, 100 epochs per task were extracted in reference to the MEG onsets. Each epoch had duration of 2 s, including 1 s of pre-onset and 1 s of post-onset. We performed the same protocol for the imagined movements in reference to the onsets of the visual and auditory stimuli. We calculated the average of 100 epochs for each bilateral movement type by using Brainstorm software. To clarify the brain activation associated with bilateral hand movements, we applied the continuous wavelet transform (Morlet wavelet) to plot the 2D time-frequency spectrogram of the average of each type of hand movement over the sensorimotor cortex area. Then, we analyzed the spatiotemporal frequency patterns over the head (not only over the sensorimotor area) by calculating the 2D time-frequency representation by using all the MEG sensors. The event-related power decreases/increases in the MEG signals were calculated after computing the 2D time-frequency spectrogram using Brainstorm functions during physical motor execution and mental motor imagery, which is a widely used technique in BMI studies. The frequency power of the event periods was averaged across 100 trials before calculating the ERD/ERS using a Morlet wavelet transform. For the SVM classification, we used a single-trial for the binary and multi-class decoding of bilateral movements using MATLAB 2016a software (Mathworks, Natick, MA, USA), which was extended to distinguish among the four classes using a multi-SVM.

D. Classification of Bilateral Hand Movements

In this study, the sensor-based BMI analysis took advantage of the event-related phenomenon observed at specific MEG sensors located over the sensorimotor cortex during real or imagined bilateral movements. To calculate the classification accuracy over all the subjects, we used binary SVM classifiers with the data from 114 MEG sensors (see Supplementary Fig. 1) after the preprocessing phase. For feature extraction, we used the MEG amplitudes of the movement-related cortical fields from single trials of 0 to 500 ms (i.e., from the EMG onset for real movements and from the presentation of the execution cue for imagined movements) for each MEG sensor around the sensorimotor cortex for each bilateral hand movement. To reduce the feature vector dimension, mean amplitude of single trial for each MEG sensor around the sensorimotor was used instead of using the whole time series which means the feature vector was the amplitude-averaged activity within the temporal segment of [0 500] ms. Thus, we calculated the average of the amplitudes in each trial during a 500-ms interval for 114 MEG sensors (the sensors were determined empirically according to the time-frequency analysis within/across subjects). A feature selection algorithm (sequential forward feature selection) was applied to avoid the high multicollinearity between the 114 values of the feature vector (see Fig. 3). We randomly split the MEG data (100 trials for each bilateral movement type) to 75% training data and 25% testing data so that the testing dataset was independent of the training dataset. Then we run 5-fold cross-validation approach in 75% of the trials in order to get the best features which refer to the most informative MEG sensors. Finally, we tested SVM model with the rest of 25% of trials. For the multi-class classification, we used two different algorithms: the hierarchical SVM algorithm [40], a decision tree with an SVM classifier at each node, and the multi-SVM (one against all [41]). We specified a Gaussian RBF kernel for the decision function of the SVM classifiers.

For the statistical analysis, two-sample t-tests were conducted to determine whether the classification accuracy significantly exceeded chance levels (50% for the 2-class

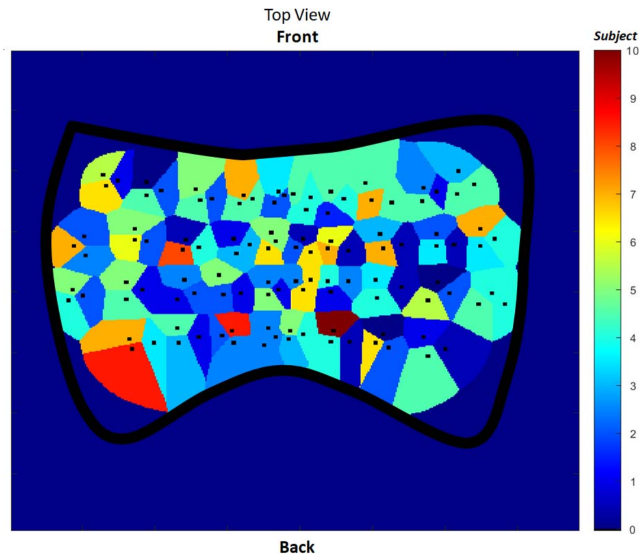

Fig. 3. Topography of the number of times a MEG sensor is selected as significant feature using sequential feature selection method for SVM classification across the cohort (114-MEG-selsected sensors surrounded by black borders were empirically selected in this study from both hemispheres above the sensorimotor cortex). See Supplementary Figure 1 for more details about MEG sensors' labels. The colormap (blue-red) is based on the number of subjects.

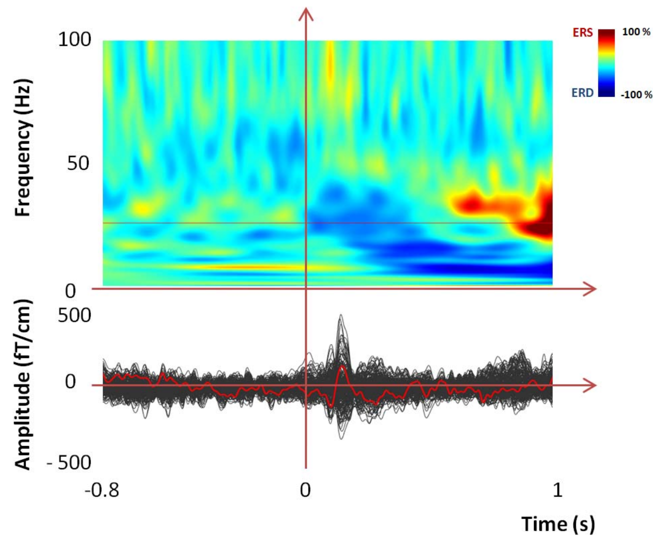

Fig. 4. An averaged waveform of a time series of 100 trials (shown in red) surrounding the motor cortex (gradiometer sensor: MEG1623) and the corresponding time-frequency representation of the movement-related oscillatory changes in a representative subject. The time window is between -800 and 1000 ms, the movement onset is at 0 ms, and the frequency band ranges from 0.5 Hz to 100 Hz. The red area in the time-frequency map indicates increases in the beta/gamma power (ERS), and the blue areas indicate decreases in the alpha power (ERD).

classification and 25% for the 4-class classification) with a threshold of $p < 0.05$. Non-parametric statistical tests, such as t-tests or two-way analysis of variance (ANOVA), and a multiple comparisons test of means using Tukey's method were used not only to confirm that the decoding performance significantly exceeded chance level but also to examine the similarities and differences in decoding between the bilateral movement types and participants and between the real and imagined movements.

III. Results

A. Time-Frequency Spectrograms of Bilateral Hand Movements by Using a Wavelet Method

To better understand brain activation related to bilateral movements, we analyzed the spatiotemporal frequency patterns by calculating the time-frequency spectrograms by using a Morlet wavelet transform at each of the MEG sensors over the sensorimotor area.

Fig. 3 shows the average of a time series of 100 trials and the corresponding time-frequency representation in a representative subject, which represents a typical waveform for a hand grasping movement using an invasive measurement (i.e., ECoG). This typical waveform was observed with most MEG sensors over the sensorimotor area while the subjects performed or imagined contralateral and ipsilateral hand movements. From the MEG time-frequency distribution (see Fig. 4), we observed clear movement-related magnetic fields, movement-related power decreases in the alpha/beta band from 0 to 0.5 s and power increases in the beta band (a clear post-movement beta rebound was observed between 0.5 and 1 s), but we did not observe any clear movement-related power increase near the high gamma band (50-100 Hz) in a single-trail level.

In addition, the movement-related power increases and decreases in the alpha and beta bands were distributed over the sensorimotor areas in both cerebral hemispheres 136 ms after the presentation of the execution cue in both bilateral voluntary hand movements and motor imagery (see Fig. 5 and Supplementary Fig. 3). Therefore, we used the spatiotemporal patterns of the low-frequencies (8–30 Hz) of MEG sensors surrounding the sensorimotor cortex to decode the type of bilateral movement.

Regarding brain activation, we observed that the frequency power did not always increase in the high gamma band while the subjects executed the predefined tasks in this MEG study, which is inconsistent with the ECoG results, in which the power of the high gamma band has been reported to increase [42]. Fig. 5 displays representative topological maps of the alpha and beta bands in four bilateral hand movements based on sensor-level analyses during motor execution. We observed clear bilateral activation surrounding the sensorimotor area during the four movement types of real and imagined movements (i.e., in the real movement, a power decrease can be observed after 136 ms and a power increase can be observed after 409 ms). The F-values of the multiple comparison tests were calculated for the representative sensor-based time-frequency map of the four classes of bilateral voluntary hand movements (see Fig. 6). Then, we calculated the group average of the sensor-based time-frequency map of the four bilateral hand classes across subjects (see Supplementary Figs. 4-11). A clear power increase/decrease was observed in the MEG sensors surrounding the sensorimotor area in all four bilateral hand classes across subjects in both real and imagined movements. Based on these observations, we selected the most relevant MEG sensors for the decoding phase.

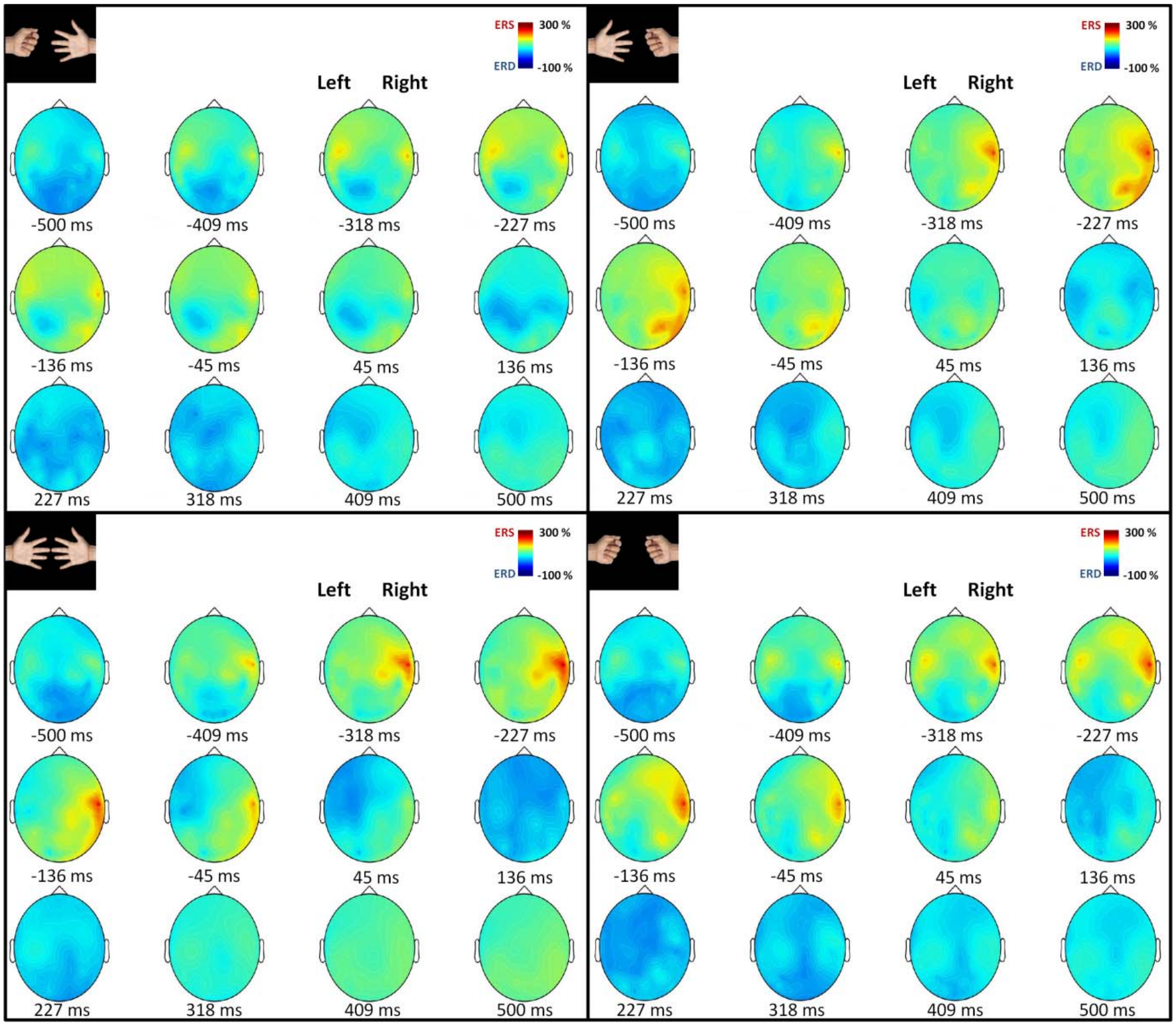

Fig. 5. A representative sensor-based time-frequency map of four classes of bilateral voluntary hand movements based on a wavelet transformation in a representative subject. The time window is between −500 and 500 ms; the movement onset is at 0 ms, and the frequency interval (alpha and beta bands) ranges from 8 Hz to 30 Hz.

Notably, the frequency topography of the bilateral movements exhibited bilateral patterns, such as an overlap between the activation of both brain hemispheres, owing to the magnetic field characteristics caused by the resulting opposite field direction in the case of opposite bilateral hand movements and the partial cancelation of the magnetic field in the case of the same bilateral movements with the presence of some hemispheric dominance due to the right- or left-handedness of the participants.

B. Single-Trial Binary Classification of Real and Imagined Bilateral Hand Movements

The average amplitudes of single-trial movement-related cortical fields from each sensor over the sensorimotor area with time windows of 0-500 ms in 8 subjects and 0-300 ms in 2 subjects were used as decoding features for classifying the four bilateral hand movements [43]. The 500-ms time window was used for subjects who showed a clear late latency component (>200 ms) of the movement-related cortical fields (see Fig. 3), while a window of 300 ms was used for subjects who did not exhibit a clear final latency component. We selected the 28 most informative MEG sensors from 114 sensors over the sensorimotor area in both hemispheres (see Fig. 3 and Supplementary Table 1).

The individual decoding accuracies for each subject on the basis of a single-trial SVM classification indicated that it was possible to discriminate the 4 types of simultaneous bilateral hand movements by using the simple combination set of 28 MEG sensors over the sensorimotor area, the given time windows and the amplitudes of movement-related cortical fields. The individual decoding accuracies varied from 60% to 85% by using all permutations of the four types of bilateral movements (i.e., a 2-class classification of contralateral and/or ipsilateral hand movements), whereas the mean decoding accuracy averaging all 6 binary combinations of the four bilateral movements across 10 participants was 74.56% (SD: 1.9) for real movement; this classification accuracy significantly exceeded the chance level of 50% with $p < 0.001$. For imagined movement, the mean decoding accuracy was

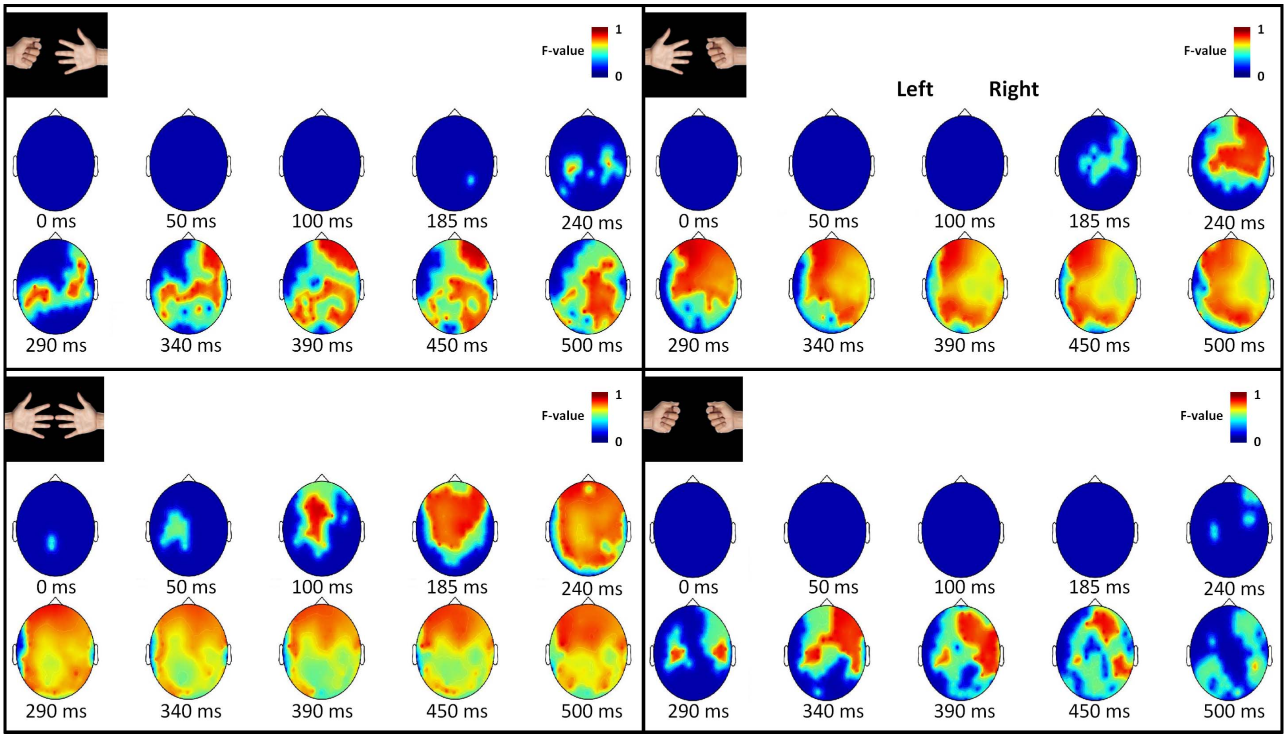

Fig. 6. F-values from multiple comparison tests of the representative sensor-based time-frequency map of four classes of bilateral voluntary hand movements. The F-values shown in this figure are color-coded on 2D discs only for p-values <0.01 using the correction type of false discovery rate (FDR). The power test was based on the magnitude, which is the square root of the frequency power. No brain activation was noticed from −500 ms to 0 s.

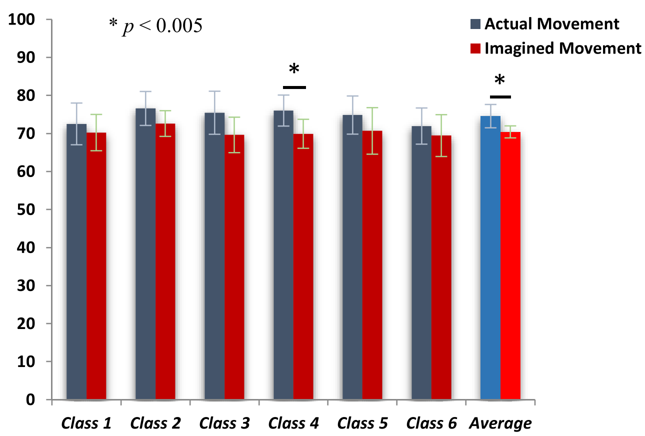

Fig. 7. Classification rate (the means ± SD), determined by using an SVM classifier, averaged across 10 participants for 6 classes of binary permutations of bilateral hand movements (R/L-Open and/or R/L-Close, R&L-Close, and R&L-Open) during performing and imagining tasks. Error bars denote the standard deviation. The green dotted line denotes a chance level of 50%. * $p < 0.005$ using non-parametric permutation tests. For each SVM classification method, the blue bars represent the classification accuracy of the actual movement, and the red bars indicate that of the imagined movement. Class 1: R-Open & L-Close vs. R-Close & L-Open, class 2: R-Open & L-Close vs. R&L-Open, class 3: R-Open & L-Close vs. R&L-Close, class 4: R-Close & L-Open vs. R&L-Open, class 5: R-Close & L-Open vs. R&L-Close, class 6: R&L-Close vs. R&L-Open.

70.41% (SD: 1.16), and this classification accuracy highly significantly exceeded the chance level of 50%.

Fig. 7 illustrates the average mean of 6 binary combinations of the four bilateral movement classes averaged across 10 participants. For class 1 (i.e., R-Open & L-Close vs. R-Close & L-Open), we obtained a mean classification of 72.51% (SD: 5.4%) and 70.23% (SD: 4.7%) for actual and imagined movements, respectively. For class 2 (i.e., R-Open & L-Close vs. R&L-Open), we obtained a mean classification accuracy of 76.57% (SD: 4.5%) and 72.61% (SD: 3.38%) for actual and imagined movements, respectively. For class 3 (i.e., R-Open & L-Close vs. R&L-Close), we obtained a mean classification accuracy of 75.45% (SD: 5.6%) and 6962% (SD: 4.66%) for actual and imagined movements, respectively. For class 4 (i.e., R-Close & L-Open vs. R&L-Open), we obtained a mean classification accuracy of 76.02% (SD: 4.1%) and 69.91% (SD: 3.81%) for actual and imagined movements, respectively. For class 5 (i.e., R-Close & L-Open vs. R&L-Close), we obtained a mean classification accuracy of 74.84% (SD: 5.1%) and 70.67% (SD: 6.12%) for actual and imagined movements, respectively. For class 6 (i.e., R&L-Close vs. R&L-Open), we obtained a mean classification accuracy of 71.55% (SD: 3.1%) and 69.44% (SD: 5.5%) for actual and imagined movements, respectively.

To examine the differences between real and imagined bilateral hand movements, we used t-tests to calculate the statistical significance of differences between the decoding accuracies of the real and imagined movements for all subjects. The results shown in Fig. 7 indicated significant differences between mean classification accuracy of real and imagined movements of all 6 classes (the value of the test statistic "$T(5) = 6.326$", p-value "$p = 0.001$") and between the real and imagined movements of class 4 ($p = 0.002$).

We used a two-way ANOVA to evaluate the decoding performance and to compare the classification results among the six classes across 10 participants. For the real movements, no significant differences were observed between participants (F(9,59) = 1.27, p = 0.28), and no significant differences were observed between classes (F(5,59) = 1.55, $p = 0.195$). Using a multiple comparisons test of the means, we observed that no classes had significantly different means, except for classes 2 and 6, the means of which were significantly different when using the Tukey-Kramer test for the type of critical value. For the imagined movements, no significant differences were observed using a two-way ANOVA between classes (F(5,59) = 0.76, p = 0.583), but we observed significant differences between participants (F(9,59) = 2.78, $p = 0.011$). These significant differences may be related to the performance of each participant on the imagery tasks. Using a multiple comparisons test of means with the Tukey-Kramer method, we observed that no classes had means that were significantly different.

C. Multi-Class Decoding of Real and Imagined Bilateral Hand Movements

Using single-trial multi-class decoding algorithms based on an SVM classifier, we sought to distinguish between the four types of bilateral hand movements. We found that the individual decoding accuracy of real movements largely exceeded the chance level (i.e., 25%), by using a hierarchical SVM (p = 1.292e-10) and a multi-SVM (p = 9.296e-10). For the imagined movements, we found that the individual decoding accuracy also exceeded the chance level, by using a hierarchical SVM (p = 9.204e-09) and a multi-SVM (p = 1.237e-07). The average decoding accuracy for all the subjects was approximately 50%, which is approximately twice the chance level in both scenarios (performing and imagining bilateral movements).

Fig. 8 shows the results of the multi-class classification of bilateral hand movements during performing and imagining tasks using two SVM algorithms. For the actual bilateral hand movements, we obtained a mean classification accuracy of 49.12% (SD: 2.36%) and 48.02% (SD: 2.81%), using the hierarchical SVM algorithm and multi-class SVM (one against all) algorithm, respectively. For the imagined bilateral hand movements, we obtained a mean classification accuracy of 42.61% (SD: 2.79%) and 39.14% (SD: 2.92%), using the hierarchical SVM algorithm and multi-class SVM (one against all) algorithm, respectively. The multi-class classification results demonstrated that there was a significant difference between the classification accuracies of the real and imagined movements, as determined by using the hierarchical SVM ($p < 0.001$) and multi-SVM ($p < 0.001$) algorithms. These results were consistent with those in [44].

For decoding the real and imagined bilateral movements, the Gaussian radial basis function (RBF) kernel SVM achieved binary classification results near the real-time BMI requirement (i.e., a classification accuracy of 70%), whereas the multi-class SVM algorithms achieved individual decoding results with a classification accuracy approximately twice the chance level. None of these results fell near or below chance level.

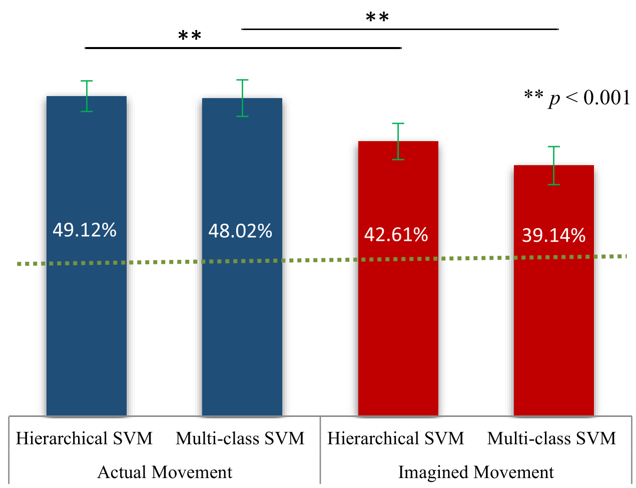

Fig. 8. Mean accuracies averaged across 10 participants for the multi-class classification of bilateral hand movements during performing and imagining tasks when using two different SVM algorithms. Error bars denote the standard deviation. The green dotted line denotes a chance level of 25%. $^{**}p < 0.001$ using non-parametric permutation tests. For each SVM classification method, the blue bars represent the classification accuracy of the actual movement, and the red bars represent that of the imagined movement.

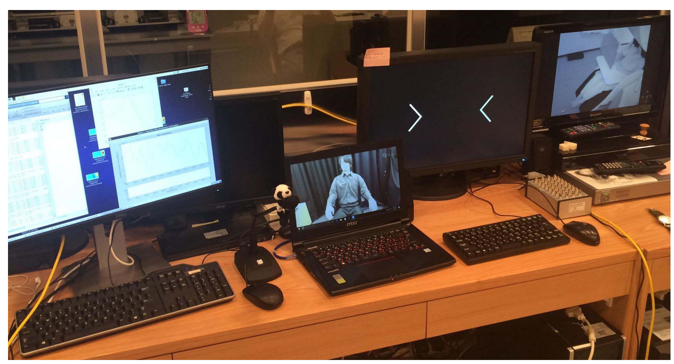

Fig. 9. Experiment setup of real-time decoding of bilateral hand movements for MEG-based brain-Geminoid interface. We can see in this picture, four screens from left to right: MEG data analysis (i.e., real-time streaming, recording and processing of multi-channel MEG data), Geminoid motion feedback using Skype, experimental paradigm interface, and MEG room feedback.

D. Real Time Control of Humanlike Robot Hands

To demonstrate the efficacy of neuromagnetic decoding of simultaneous bilateral hand movements in real world applications, we controlled a human-like android robot (Geminoid HI-2) by sending commands from Osaka city to Kyoto city in Japan. The implementation of the control application was divided into three modules, the MEG signal acquisition, decoding module and the Geminoid control module. MEG signals were recorded every 1 s using real-time FieldTrip toolbox, the classification algorithm module was implemented in MATLAB, and the Geminoid control module (control's logic) was implemented using Java language. The last two modules interfaced with each other via TCP/IP protocol (see Fig. 9).

In these real-time tests, two subjects were asked to perform real-time control of humanlike robot hands with four commands based on their four bilateral hand movements (see Supplementary Video). For calibration phase, the participants achieved an average accuracy of 73% for contralateral hand movements and 77.75% for ipsilateral hand movements. For real-time voluntary movements test, the participants demonstrated reliable control of the humanlike robot hands, achieving an average accuracy of 61.25% for contralateral hand movements and 63.5% for ipsilateral hand movements using 80 single-trials for each class for evaluation. For motor imagery, a mean classification accuracy of 58.75% and 59.5% were obtained for contralateral and ipsilateral hand movements, respectively.

IV. Discussion

All previous studies have decoded unilateral movements, such as right or left hand/finger/toe grasping, and tongue motions during real and imagined movements to achieve a practical real-time BMI control [11]–[17]. These types of unilateral BMI tasks are not suitable for the development of multidimensional BMI systems that require higher dimensional control and more naturalistic BMI tasks such as bilateral arm/hand/finger movements [23]. The present study investigated decoding the multi-class simultaneous bilateral hand movements of a subject in the context of a noninvasive multidimensional BMI for both voluntary control and motor imagery situations. We analyzed and decoded the sensorimotor activity associated with four types of bilateral hand movements, as determined using neuromagnetic event-related modulation, to obtain proof-of-concept evidence for multidimensional BMI applications. To our knowledge, no previous studies have investigated the analysis and classification of 4 types of bilateral hand movements by using noninvasive measurements.

Using sensor-based maps of magnetic fields and frequency power, we found that the spatiotemporal distributions of neuromagnetic fields and oscillatory changes exhibited strong bilateral activation with high ipsilateral activation at 136 ms around the sensorimotor cortex (see Figs. 4 and 5). We observed decreases in the frequency power in the beta and alpha bands when the participant performs or imagines bilateral hand movements. These results were consistent with those from previous studies that have reported the brain activation associated with bilateral hand/finger movements [22], [24]–[26], [45]. Therefore, we were able to use single-trial amplitudes of the 28 MEG signals over the sensorimotor area as characteristics, because these data carried sufficient spatiotemporal patterns to distinguish all 4 types of bilateral hand movements.

In this study, for the binary classification of four types of simultaneous contralateral and ipsilateral hand movements that were performed during neuromagnetic measurements, we achieved a mean classification accuracy of approximately 70% (i.e., the minimum accuracy requirement for reliable BMI control [46]), by using single trials to decode real and imagined bilateral hand movements. This decoding accuracy demonstrated that the proposed multidimensional BMI paradigm is promising for real-time continuous and multidimensional control applications, in contrast to previous studies that have classified unilateral movements, such as grasping, and the rest state [11]–[19]. In addition, uni- and bi-lateral hand movements can be combined to build a multidimensional BMI system with more than seven commands, including the rest state.

In the present study, we also obtained a decoding accuracy for a multi-class classification using two SVM algorithms that was significantly higher than the chance level (25%). The multi-class classification results in this paper are promising and are comparable to those of previous studies that have reported different multi-class BMI paradigms [20]–[23]. In addition, use of advanced machine learning algorithms such as deep learning methods or increasing the number of trial repetitions (i.e., the decision rule based on a loop) instead of using a single-trial SVM classification may increase the classification accuracy. However, complex classification algorithms are a drawback for a practical BMI, because these approaches are generally slower than other classifiers. In most cases, complex algorithms require a very large amount of training data and are not sufficiently fast for real-time BMI applications. A major limitation of the proposed BMI approach is that it is subject-specific BMI, which requires individual data calibration regularly and system training. It is still difficult to overcome all of the limitations of BMI based on mental motor imagery due to kinematic imagination variability and the effects of practice. During physical motor execution, it is desirable to use some compatible gloves to record precisely the reaction times (RT) and movement kinematics (e.g. movement velocity and range).

As noted above, the present MEG experiments sought to provide a conceptual advancement and proof-of-concept. Notably, being able to decode bilateral hand movements is an important step toward understanding dual-task characteristics, thereby leading to enhanced multidimensional BMI control and performance. In summary, we used a single-trial SVM classification to distinguish among four types of bilateral hand movements by using MEG measurements in two scenarios: motor execution and motor imagery. Regarding brain activation, the sensorimotor cortex showed discriminative time-series signals and power frequency distributions in bilateral hemispheres according to the four tasks. In addition, our decoding results demonstrated the potential utility of bilateral hand movement decoding for engineering purposes such as multidimensional BMI control. Although further studies are required, our decoding results suggested that our BMI protocol may enhance human multitasking ability through the use of multidimensional brain-controlled prosthetic devices.

Author Contributions

ANB and MH designed the study and performed experiments, analyses, and literature review, and ANB developed experimental programs and drafted the manuscript. MH, HI, SN and TS performed the interventions, supervised the research and revised the manuscript. All of the authors reviewed and approved the manuscript.

Declaration of Conflicting Interests

The authors declared no potential conflicts of interest with respect to the research, and publication of this article.

References

[1] G. Pfurtscheller, C. Neuper, and J. Kalcher, “40-Hz oscillations during motor behavior in man,” *Neurosci. Lett.*, vol. 164, pp. 179–182, Dec. 1993.

[2] G. Pfurtscheller, C. Brunner, A. Schlögl, and F. H. Lopes da Silva, “Mu rhythm (de)synchronization and EEG single-trial classification of different motor imagery tasks,” *NeuroImage*, vol. 31, no. 1, pp. 153–159, 2006.

[3] C. Neuper, G. R. Müller-Putz, R. Scherer, and G. Pfurtscheller, “Motor imagery and EEG-based control of spelling devices and neuroprostheses,” *Prog. Brain Res.*, vol. 159, pp. 393–409, 2006, doi: 10.1016/S0079-6123(06)59025-9.

[4] T. M. Vaughan *et al.*, “The wadsworth BCI research and development program: At home with BCI,” *IEEE Trans. Neural Syst. Rehabil. Eng.*, vol. 14, no. 2, pp. 229–233, Jun. 2006.

[5] J. R. Wolpaw, N. Birbaumer, D. J. McFarland, G. Pfurtscheller, and T. M. Vaughan, “Brain–computer interfaces for communication and control,” *Clin. Neurophysiol.*, vol. 113, pp. 767–791, Jun. 2002.

[6] N. Birbaumer, “Breaking the silence: Brain–computer interfaces (BCI) for communication and motor control,” *Psychophysiology*, vol. 43, pp. 517–532, Nov. 2006.

[7] B. Blankertz, G. Dornhege, M. Krauledat, K.-R. Müller, and G. Curio, “The non-invasive berlin brain–computer interface: Fast acquisition of effective performance in untrained subjects,” *NeuroImage*, vol. 37, pp. 539–550, Aug. 2007.

[8] R. Fukuma *et al.*, “Closed-loop control of a neuroprosthetic hand by magnetoencephalographic signals,” *PLoS ONE*, vol. 10, p. e0131547, Jul. 2015.

[9] R. Fukuma *et al.*, “Real-time control of a neuroprosthetic hand by magnetoencephalographic signals from paralysed patients,” *Sci. Rep.*, vol. 6, Feb. 2016, Art. no. 21781.

[10] L. R. Hochberg *et al.*, “Neuronal ensemble control of prosthetic devices by a human with tetraplegia,” *Nature*, vol. 442, no. 7099, pp. 164–171, Jul. 2006.

[11] G. Pfurtscheller, “Enhancement of sensorimotor rhythms with motor imagery,” *Appl. Psychophysiol. Biofeedback*, vol. 31, p. 351, Dec. 2006.

[12] G. Pfurtscheller and C. Neuper, “Future prospects of ERD/ERS in the context of brain–computer interface (BCI) developments,” *Event-Rel. Dyn. Brain Oscillations*, vol. 159, pp. 433–437, 2006.

[13] F. Popescu, S. Fazli, Y. Badower, B. Blankertz, and K.-R. Müller, “Single trial classification of motor imagination using 6 Dry EEG electrodes,” *PLoS ONE*, vol. 2, p. e637, Jul. 2007.

[14] L. R. Hochberg *et al.*, “Reach and grasp by people with tetraplegia using a neurally controlled robotic arm,” *Nature*, vol. 485, pp. 372–375, May 2012.

[15] J. L. Collinger *et al.*, “High-performance neuroprosthetic control by an individual with tetraplegia,” *Lancet*, vol. 381, pp. 557–564, Feb. 2013.

[16] T. Yanagisawa *et al.*, “Real time cortical control of a prosthetic hand using electrocorticogram (ECoG),” *Neurosci. Res.*, vol. 65, p. S49, Jan. 2009.

[17] T. Yanagisawa *et al.*, “Real-time control of a prosthetic hand using human electrocorticography signals,” *J. Neurosurg.*, vol. 114, pp. 1715–1722, Jun. 2011.

[18] L. Qin, L. Ding, and H. He, “Motor imagery classification by means of source analysis for brain computer interface applications,” *J. Neural Eng.*, vol. 2, pp. 65–72, Dec. 2004.

[19] A. Vallabhaneni and B. He, “Motor imagery task classification for brain computer interface applications using spatiotemporal principle component analysis,” *Neurol. Res.*, vol. 26, pp. 282–287, Apr. 2004.

[20] H. Sugata *et al.*, “Neural decoding of unilateral upper limb movements using single trial MEG signals,” *Brain Res.*, vol. 1468, pp. 29–37, Aug. 2012.

[21] K. LaFleur, K. Cassady, A. Doud, K. Shades, E. Rogin, and B. He, “Quadcopter control in three-dimensional space using a noninvasive motor imagery-based brain–computer interface,” *J. Neural Eng.*, vol. 10, no. 4, p. 046003, Aug. 2013.

[22] M. Nakamura *et al.*, “Categorical discrimination of human body parts by magnetoencephalography,” *Frontiers Hum. Neurosci.*, vol. 9, p. 609, Nov. 2015.

[23] J. Meng, S. Zhang, A. Bekyo, J. Olsoe, B. Baxter, and B. He, “Noninvasive electroencephalogram based control of a robotic arm for reach and grasp tasks,” *Sci. Rep.*, vol. 6, Dec. 2016, Art. no. 38565.

[24] L. Deecke *et al.*, “Hemispherical differences of cerebral potentials preceding right and left unilateral and bilateral finger movements in right-handed subjects,” *Pflügers Arch.-Eur. J. Physiol.*, p. R74, Mar. 1978.

[25] R. Kristeva, E. Keller, L. Deecke, and H. H. Kornhuber, “Cerebral potentials preceding unilateral and simultaneous bilateral finger movements,” *Electroencephalogr. Clin. Neurophysiol.*, vol. 47, no. 2, pp. 229–238, 1979.

[26] R. Kristeva, D. Cheyne, W. Lang, G. Lindinger, and L. Deecke, “Movement-related potentials accompanying unilateral and bilateral finger movements with different inertial loads,” *Electroencephalogr. Clin. Neurophysiol.*, vol. 75, pp. 410–418, May 1990.

[27] R. Kristeva, D. Cheyne, and L. Deecke, “Neuromagnetic fields accompanying unilateral and bilateral voluntary movements: Topography and analysis of cortical sources,” *Electroencephalogr. Clin. Neurophysiol.*, vol. 81, pp. 284–298, Aug. 1991.

[28] R. Kristeva, D. Cheyne, and L. Deecke, “Human neuromagnetic fields associated with unilateral and bilateral voluntary movements,” *Int. J. Psychophysiol.*, vol. 11, pp. 48–49, Jul. 1991.

[29] A. R. Luft *et al.*, “Repetitive bilateral arm training and motor cortex activation in chronic stroke: A randomized controlled trial,” *JAMA*, vol. 292, pp. 1853–1861, Oct. 2004.

[30] H. Sugata *et al.*, “Alpha band functional connectivity correlates with the performance of brain–machine interfaces to decode real and imagined movements,” *Frontiers Hum. Neurosci.*, vol. 8, p. 620, Aug. 2014.

[31] A. Ikeda *et al.*, “Movement-related potentials associated with bilateral simultaneous and unilateral movements recorded from human supplementary motor area,” *Electroencephalogr. Clin. Neurophysiol.*, vol. 95, pp. 323–334, Nov. 1995.

[32] J. Diedrichsen, T. Wiestler, and J. W. Krakauer, “Two distinct ipsilateral cortical representations for individuated finger movements,” *Cerebral Cortex*, vol. 23, pp. 1362–1377, Jun. 2013.

[33] T. Wu, L. Wang, M. Hallett, K. Li, and P. Chan, “Neural correlates of bimanual anti-phase and in-phase movements in Parkinson’s disease,” *Brain*, vol. 133, pp. 2394–2409, Aug. 2010.

[34] A. Guillot, F. Di Rienzo, T. MacIntyre, A. Moran, and C. Collet, “Imagining is not doing but involves specific motor commands: A review of experimental data related to motor inhibition,” *Frontiers Hum. Neurosci.*, vol. 6, p. 247, Sep. 2012.

[35] L. Kauhanen *et al.*, “EEG and MEG brain-computer interface for tetraplegic patients,” *IEEE Trans. Neural Syst. Rehabil. Eng.*, vol. 14, no. 2, pp. 190–193, Jun. 2006.

[36] S. Lehericy *et al.*, “Correspondence between functional magnetic resonance imaging somatotopy and individual brain anatomy of the central region: Comparison with intraoperative stimulation in patients with brain tumors,” *J. Neurosurg.*, vol. 92, pp. 589–598, Apr. 2000.

[37] C. D. Alberstone *et al.*, “Magnetic source imaging and brain surgery: Presurgical and intraoperative planning in 26 patients,” *J. Neurosurg.*, vol. 92, pp. 79–90, Jan. 2000.

[38] P. Hlustík, A. Solodkin, R. P. Gullapalli, D. C. Noll, and S. L. Small, “Somatotopy in human primary motor and somatosensory hand representations revisited,” *Cerebral Cortex*, vol. 11, pp. 312–321, Apr. 2001.

[39] F. Tadel, S. Baillet, J. C. Mosher, D. Pantazis, and R. M. Leahy, “Brainstorm: A user-friendly application for MEG/EEG analysis,” *Comput. Intell. Neurosci.*, vol. 2011, no. 2011, pp. 879716-1–879716-13, 2011.

[40] E. Dong *et al.*, “Classification of multi–class motor imagery with a novel hierarchical SVM algorithm for brainâŁ“computer interfaces,” *Med. Biol. Eng. Comput.*, vol. 55, no. 10, pp. 1809–1818, 2017.

[41] L. Bottou *et al.*, “Comparison of classifier methods: A case study in handwritten digit recognition,” in *Proc. 12th IAPR Int. Conf. Pattern Recognit. Conf. B, Pattern Recognit. Neural Netw.*, vol. 2, 1994, pp. 77–82.

[42] K. J. Miller, G. Schalk, E. E. Fetz, M. den Nijs, J. G. Ojemann, and R. P. N. Rao, “Cortical activity during motor execution, motor imagery, and imagery-based online feedback,” *Proc. Nat. Acad. Sci. USA*, vol. 107, pp. 4430–4435, Mar. 2010.

[43] H. Sugata *et al.*, “Movement-related neuromagnetic fields and performances of single trial classifications,” *Neuroreport*, vol. 23, pp. 16–20, Jan. 2012.

[44] H. Sugata, M. Hirata, T. Yanagisawa, K. Matsushita, S. Yorifuji, and T. Yoshimine, “Common neural correlates of real and imagined movements contributing to the performance of brain–machine interfaces,” *Sci. Rep.*, vol. 6, Apr. 2016, Art. no. 24663.

[45] W. Yi, S. Qiu, H. Qi, L. Zhang, B. Wan, and D. Ming, “EEG feature comparison and classification of simple and compound limb motor imagery,” *J. Neuroeng. Rehabil.*, vol. 10, p. 106, Oct. 2013.

[46] G. Pfurtscheller *et al.*, “Human brain-computer interface,” in *Motor Cortex in Voluntary Movements: A Distributed System for Distributed Functions* (Frontiers in Neuroscience), E. Vaadia and A. Riehle, Eds. Boca Raton, FL, USA: CRC Press, 2005, pp. 405–441.